Correlated electron dynamics in nonsequential double ionization of molecules by mid-infrared fields

Qingbin Tang,[1] **Yueming Zhou,**[1,3] **Cheng Huang,**[1] **Qing Liao,**[1] **and Peixiang Lu,**[1,2,*]

[1]*Wuhan National Laboratory for Optoelectronics and School of Physics, Huazhong University of Science and Technology, Wuhan 430074, China*
[2]*Key Laboratory of Fundamental Physical Quantities Measurement of Ministry of Education, Wuhan, 430074, China*
[3]*zhouymhust@gmail.com*
[*]*lupeixiang@mail.hust.edu.cn*

Abstract: The electron dynamics in strong field nonsequential double ionization (NSDI) of nitrogen molecules by mid-infrared (MIR) laser pulses is investigated with the three-dimensional classical ensemble model. The numerical results show that in the MIR regime, the correlated behavior of the two electrons from NSDI is independent on the molecular alignment, contrary to the case in the near-infrared (NIR) regime where the electron correlations exhibit a strong alignment dependence. In consistent with the experimental results, our numerical results show that the longitudinal momentum spectrum of the doubly charged ion evolves from a wide single-hump structure at NIR regime into a double-hump structure when wavelength enters the MIR regime. This double-hump structure becomes more pronounced as the wavelength further increases. The responsible microscopic electron dynamics of NSDI at the MIR regime is explored by back analysis of the classical trajectories.

OCIS codes: (020.4180) Multiphoton; (260.3230) Ionization; (270.6620) Strong-field process.

References and links

1. D. N. Fittinghoff, P. R. Bolton, B. Chang, and K. C. Kulander, "Observation of nonsequential double ionization of helium with optical tunneling," Phys. Rev. Lett. **69,** 2642-2645 (1992).
2. B. Walker, B. Sheehy, L. F. Dimauro, P. Agostini, K. J. Schafer, and K. C. Kulander, "Precision measurement of strong field double ionizaiton of helium," Phys. Rev. Lett. **73,** 1227-1230 (1994).
3. Th. Weber, H. Giessen, M. Weckenbrock, G. Urbasch, A. Staudte, L. Spielberger, O. Jagutzki, V. Mergel, M. Vollmer, and R. Dörner, "Correlated electron emmision in multiphoton double ionization," Nature (London) **405,** 658-661 (2000).
4. B. Feuerstein, R. Moshammer, D. Fischer, A. Dorn, C. D. Schröter, J. Deipenwisch, J. R. Crespo Lopez-Urrutia, C. Höhr, P. Neumayer, J. Ullrich, H. Rottke, C. Trump, M. Wittmann, G. Korn, and W. Sandner, "Separation of recollision mechanisms in nonsequential strong field double ionizaion of Ar: the role of excitation tunneling," Phys. Rev. Lett. **87,** 043003 (2001).
5. Y. Zhou, Q. Liao, and P. Lu, "Mechanism for high-energy electrons in nonsequential double ionization below the recollision-excitation threshold," Phys. Rev. A **80,** 023412 (2009).
6. Q. Liao, Y. Zhou, C. Huang, and P. Lu, "Multiphoton Rabi oscillations of correlated electrons in strong-field nonsequential double ionization," New J. Phys. **14,** 013001 (2012).
7. M. Weckenbrock, D. Zeidler, A. Staudte, Th. Weber, M. Schöffler, M. Meckel, S. Kammer, M. Smolarski, O. Jagutzki, V. R. Bhardwaj, D. M. Rayner, D. M. Villeneuve, P. B. Corkum, and R. Dörner, "Fully differential rates for femtosecond multiphoton double ionization of neon," Phys. Rev. Lett. **92,** 213002 (2004).

#171495 - $15.00 USD Received 29 Jun 2012; revised 3 Aug 2012; accepted 6 Aug 2012; published 10 Aug 2012

8. A. Rudenko, K. Zrost, B. Feuerstein, V. L. B. de Jesus, C. D. Schröter, R. Moshammer, and J. Ullrich, "Correlated multielectron dynamics in ultrafast laser pulse interactions with atoms," Phys. Rev. Lett. **93,** 253001 (2004).
9. A. Staudte, C. Ruiz, M. Schöffler, S. Schössler, D. Zeidler, Th. Weber, M. Meckel, D. M. Villeneuve, P. B. Corkum, A. Becker, and R. Dörner, "Binary and recoil collisions in strong field double ionization of helium," Phys. Rev. Lett. **99,** 263002 (2007).
10. Y. Zhou, C. Huang, Q. Liao, W. Hong, and P. Lu, "Control the revisit time of the electron wave packet" Opt. Lett. **36,** 2758-2760 (2011).
11. R. Kopold, W. Becker, H. Rottke, and W. Sandner, "Routes to nonsequential double ionization," Phys. Rev. Lett. **85,** 3781-3784 (2000).
12. A. Becker, R. Dörner, and R. Moshammer, "Multiple fragmentation of atoms in femtosecond laser pulses," J. Phys. B **38,** S753-S772 (2005).
13. M. Lein, E. K. U. Gross, and V. Engel, "Intense-field double ionization of helium: identifying the mechanism," Phys. Rev. Lett. **85,** 4707-4710 (2000).
14. Y. Zhou, Q. Liao, and P. Lu, "Asymmetric electron energy sharing in strong-field double ionization of helium," Phys. Rev. A **82,** 053402 (2010).
15. S. L. Haan, L. Breen, A. Karim, and J. H. Eberly, "Variable time lag and backward ejection in full-dimensional analysis of strong-field double ionization," Phys. Rev. Lett. **97,** 103008 (2006).
16. Q. Liao, P. X. Lu, Q. B. Zhang, W. Y. Hong, and Z. Y. Yang, "Phase-dependent nonsequential double ionization by few-cycle laser pulses," J. Phys. B **41,** 125601 (2008).
17. Y. Zhou, C. Huang, A. H. Tong, Q. Liao, and P. Lu, "Correlated electron dynamics in nonsequential double ionization by orthogonal two-color laser pulses," Opt. Express **19,** 2301-2308 (2011).
18. P. B. Corkum, "Plasma perspective on strong-field multiphoton ionization," Phys. Rev. Lett. **71,** 1994-1997 (1993).
19. K. J. Schafer, B. Yang, L. F. DiMauro, and K. C. Kulander, "Above threshold ionization beyond the high harmonic cutoff," Phys. Rev. Lett. **70,** 1599-1602 (1993).
20. P. Agostini, and L. F. DiMauro, "Atoms in high intensity mid-infrared pulses," Contemp. Phys. **49,** 179-197 (2008).
21. C. I. Blaga, F. Catoire, P. Colosimo, G. G. Paulus, H. G. Muller, P. Agostini, and F. Dimauro, "Srong-field photoionization revisited," Nat. phys. **5,** 335-338 (2009).
22. W. Quan, Z. Lin, M. Wu, H. Kang, H. Liu, X. Liu, J. Chen, J. Liu, X. T. He, S. G. Chen, H. Xiong, L. Guo, H. Xu, Y. Fu, Y. Cheng, and Z. Z. Xu, "Classical aspects in above-threshold ionization with a midinfrared strong laser field," Phys. Rev. Lett. **103,** 093001 (2009).
23. P. Colosimo, G. Doumy, C. I. Blaga, J. Wheeler, C. Hauri, F. Catoire, J. Tate, R. Chirla, A. M. March, G. G. Paulus, H. G. Muller, P. Agostini, and L. F. Dimauro, "Scaling strong-field interactions towards the classical limit," Nat. Phys. **4,** 386-389 (2008).
24. G. Doumy, J. Wheeler, C. Roedig, R. Chirla, P. Agostini, and L. F. DiMauro, "Attosecond synchronization of high-order harmonics from midinfrared drivers," Phys. Rev. Lett. **102,** 093002 (2009).
25. A. S. Alnaser, D. Comtois, A. T. Hasan, D. M. Villeneuve, J-C. Kieffer, and I. V. Litvinyuk, "Strong-field non-sequential double ionization: wavelength dependence of ion momentum distributions for neon and argon," J. Phys. B **41,** 031001 (2008).
26. O. Herrwerth, A. Rudenko, M. Kremer, V. L. B. de Jesus, B. Fischer, G. Gademann, K. Simeonidis, A. Achtelik, Th. Ergler, B. Feuerstein, C. D. Schröter, R. Moshammer, and J. Ullrich, "Wavelength dependence of sub-lasercycle few-electron dynamics in strong-field multiple ionization," New J. Phys. **10,** 025007 (2008).
27. A. D. DiChiara, E. Sistrunk, C. I. Blaga, U. B. Szafruga, P. Agostini, and L. F. DiMauro, "Inelastic scattering of broadband electron wave packets driven by an intense midinfrared laser field," Phys. Rev. Lett. **108,** 033002 (2012).
28. D. Zeidler, A. Staudte, A. B. Bardon, D. M. Villeneuve, R. Dörner, and P. B. Corkum, "Controlling attosecond double ionization dynamics via molecular alignment," Phys. Rev. Lett. **95,** 203003 (2005).
29. C. Huang, Y. Zhou, A. H. Tong, Q. Liao, W. Hong, and P. Lu, "The effect of molecular alignment on correlated electron dynamics in nonsequential double ionization," Opt. Express **19,** 5627-5634 (2011).
30. Y. Zhou, C. Huang, Q. Liao, and P. Lu, "Classical simulations including electron correlations for sequential double ionization," Phys. Rev. Lett. **109,** 053004 (2012).
31. K. Sacha, and B. Eckhardt, "Pathways to double ionization of atoms in strong fields," Phys. Rev. A **63,** 043414 (2001).
32. Y. Zhou, Q. Liao, and P. Lu, "Complex sub-laser-cycle electron dynamics in strong-field nonsequential triple ionizaion," Opt. Express **18,** 16025-16034 (2010).
33. S. L. Haan, Z. S. Smith, K. N. Shomsky, and P. W. Plantinga, "Electron drift directions in strong-field double ionization of atoms," J. Phys. B **42,** 134009 (2009).
34. Y. Zhou, Q. Liao, Q. Zhang, W. Hong, and P. Lu, "Controlling nonsequential double ionization via two-color few-cycle pulses," Opt. Express **18,** 632-638 (2010).
35. S. L. Haan, J. S. Van Dyke, and Z. S. Smith, "Recollision excitation, electron correlation, and the production of high-momentum electrons in double ionization," Phys. Rev. Lett. **101,** 113001 (2008).

#171495 - $15.00 USD Received 29 Jun 2012; revised 3 Aug 2012; accepted 6 Aug 2012; published 10 Aug 2012

36. C. Figueira de Morisson Faria, T. Shaaran, X. Liu, and W. Yang, "Quantum interference in laser-induced nonsequential double ionization in diatomic molecules: Role of alignment and orbital symmetry," Phys. Rev. A **78,** 043407 (2008).
37. T. Shaaran, B. B. Augstein, and C. Figueira de Morisson Faria, "Excitation two-center interference and the orbital geometry in laser-induced nonsequential double ionization of diatomic molecules," Phys. Rev. A **84,** 013429 (2011).
38. X. Y. Jia, W. D. Li, J. Fan, J. Liu, and J. Chen, " Suppression effect in the nonsequential double ionization of molecules by an intense laser field," Phys. Rev. A **77,** 063407 (2008).
39. X. Y. Jia, W. D. Li, J. Liu, and J. Chen, "Alignment-dependent nonsequential double ionization of N_2 in intense laser fields: The role of different valence orbitals" Phys. Rev. A **80,** 053405 (2009).
40. E. Eremina, X. Liu, H. Rottke, W. Sandner, M. G. Schätzel, A. Dreischuh, G. G. Paulus, H. Walther, R. Moshammer, and J. Ullrich, "Influence of molecular structure on double ionization of N_2 and O_2 by high intensity ultrashort laser pulses," Phys. Rev. Lett. **92,** 173001 (2004).
41. X. Liu, C. Figueira de Morisson Faria, W. Becker, and P. B. Corkum, "Attosecond electron thermalization by laser-driven electron recollision in atoms," J. Phys. B **39,** L305-L311 (2006).

1. Introduction

Nonsequential double ionization (NSDI) is a fundamental process in laser-matter interaction. Due to the strongly correlated electron-electron behavior, NSDI have attracted increasing attention since the observation of the knee structure in the ion yield versus laser intensity curve [1]. A series of experimental and theoretical studies [2-17] have provided convincing evidences that the quasiclassical recollision model is responsible for NSDI [18, 19]. According to this model, the first electron tunnels through the combined barrier of the laser electric field and the Coulomb potential. Then it is driven by the oscillating electric field and returns to the parent ion as the electric field reverses its direction, recolliding with the ion inelastically and leading to the second electron freed directly in an (e, 2e) process or excited with subsequent field ionization (RESI) [4].

Partly due to the limitation of ultrafast amplifier technology, the wavelengths of the laser pulse in those previous studies are mainly in the NIR region ($\lambda \leq 1\mu m$). With the advance of ultrafast laser technology, the MIR laser pulse ($1\mu m < \lambda \leq 10\mu m$) have become available [20]. Recently, the interaction of atoms and molecules with MIR laser fields has drew much attention and new phenomena and new applications have been observed and proposed [21-24]. For example, an unexpected spike-like structure at the low energy of the above-threshold-ionization (ATI) spectra in the MIR regime has been experimentally observed [21, 22]. In the study of high-harmonic generation (HHG), it has shown that the MIR laser pusle not only produces much more energetic harmonic photons but also reduces harmonic chirps [24], which is beneficial for attosecond pulse generation. The strong-field NSDI of atoms and molecules by the MIR pulses has also attracted experimental attention [25-27]. For instance, In Refs. [25, 26], it has been shown that the shape of longitudinal momentum distributions of the doubly charged ion for atoms and molecules shows a double-hump structure in the MIR regime, different from the case in the NIR regime where it is a single-hump structure. This double-hump becomes more pronounced as the wavelength further increases [25, 26].

The previous investigations [28, 29] have shown that in the NIR regime, the electron correlation of the electron pairs from NSDI strongly depends on the molecular alignment. For instance, the electron pairs from NSDI of N_2 by the 800-*nm* pulses are more likely to emit into the same hemisphere when the molecular axis is aligned along the laser polarization. In this paper, with the 3D fully classical ensemble model [15], we investigate the correlated electron dynamics in NSDI of N_2 by the MIR laser pulses. Our numerical result shows that the correlated behavior of the electron pairs from NSDI is independent on the molecular alignment in the MIR regime, contrary to the case in the NIR regime [28]. Our results show that the longitudinal momentum spectrum of the doubly charged ion evolves from a wide single-hump

#171495 - $15.00 USD Received 29 Jun 2012; revised 3 Aug 2012; accepted 6 Aug 2012; published 10 Aug 2012

structure at NIR regime into a double-hump structure when wavelength enters the MIR regime. This double-hump structure becomes more pronounced as the wavelength further increases. This behavior agrees well with the experimental observations [25, 26]. Back analysis reveals that the recollision ionization (RCI) is strongly enhanced with the increasing wavelength. This RCI mechanism dominates NSDI for both alignments at the MIR regime, and thus for both alignments the electron pairs involved in NSDI are more likely to escape into the same hemisphere, leading to the alignment-independent electron correlations. Additionally, the intensity dependence of longitudinal momentum distributions of the doubly charged ion is discussed.

2. The classical ensemble model

Due to the huge computational demand of describing the two-electron system in the strong laser field, current theoretical efforts have resorted to classical methods [15, 30, 31]. Here we employ the classical model introduced by Eberly *et al* to investigation NSDI of N_2. This classical model has been successful in understanding of NSDI before [14, 32-35]. The evolution of the system in this model is determined by the classical equation of motion $d^2\mathbf{r}_i/dt^2 = -\mathbf{E}(\mathrm{t}) - \nabla[V_{ne}(\mathbf{r}_i) + V_{ee}(\mathbf{r}_1, \mathbf{r}_2)]$, where the subscript i is the label of the two different electrons and $\mathbf{E}(t)$ is the linearly polarized electric field. The nucleus-electron and electron-electron interaction are represented by a 3D soft-Coulomb potential $V_{ne} = -1/\sqrt{(\mathbf{r}_1 + R/2)^2 + a^2} - 1/\sqrt{(\mathbf{r}_1 - R/2)^2 + a^2} - 1/\sqrt{(\mathbf{r}_2 + R/2)^2 + a^2} - 1/\sqrt{(\mathbf{r}_2 - R/2)^2 + a^2}$ and $V_{ee} = 1/\sqrt{(\mathbf{r}_1 - \mathbf{r}_2)^2 + b^2}$, respectively. To obtain the initial value, the ensemble is populated starting from a classically allowed position for the N_2 ground state energy of -1.67 a.u. The available kinetic energy is distributed between the electrons randomly. Then the electrons are allowed to evolve a sufficient long time in the absence of the laser field to obtain stable position and momentum distributions [5, 17, 33]. To avoid autoionization and ensure stability, we set the screening parameter a and b to be 1.15 a.u. and 0.05 a.u., respectively. In the present calculations, the internuclear distance R is set to be 2.0 a.u (the internuclear distance of N_2). The electric field $\mathbf{E}(t)$ is linearly polarized along the z axis. The pulse has a trapezoidal shape with two-cycle turn on, six cycles at full strength, and two-cycle turn off. After the laser pulse is turned off, we determine double ionization (DI) if both electrons achieve positive energy.

Note that the classical model can not describe the interference and orbital symmetry effect. It has been shown that for the molecules the two-center interference and the orbital geometry play important roles in NSDI [36-39]. For example, with the S-matrix theory it has been shown that for NSDI of N_2 the alignment-dependent contributions from the outmost and the suboutmost orbits are different [39]. In ref. [37] it has been shown that the correlated electron momentum distributions for NSDI of diatomic molecules exhibit interference structure, which is due to the orbit geometry and two-center interference. Of course, these quantum effects could not be captured by classical models. Investigations on these effects must resort to quantum models, for example, the well developed S-matrix theory [36-39]. For the issues this paper focused, the classical model has been proved to be valid [29]. Thus, in this paper, we employ the classical model for simplicity and to provide intuitive insight into the physical process.

3. Results and discussions

Figure 1 displays the correlated electron momentum distributions in the direction of the laser polarization at the intensity of $1.0 \times 10^{14} W/cm^2$ with the wavelengthes of 800 *nm* (the first row), 1200 nm (the second row) and 1600 nm (the third row). In Figs. 1(a), 1(c) and 1(e) the molecular axis is aligned parallel to the laser polarization while in Figs. 1(b), 1(d) and 1(f) the molecular axis is perpendicular to the laser polarization. For the 800-*nm* pulses, the electron correlations strongly depend on the alignment of the molecules, as shown in Figs. 1(a) and 1(b). Compared with parallel molecules, the electron pairs are more likely to emit into the

#171495 - $15.00 USD Received 29 Jun 2012; revised 3 Aug 2012; accepted 6 Aug 2012; published 10 Aug 2012

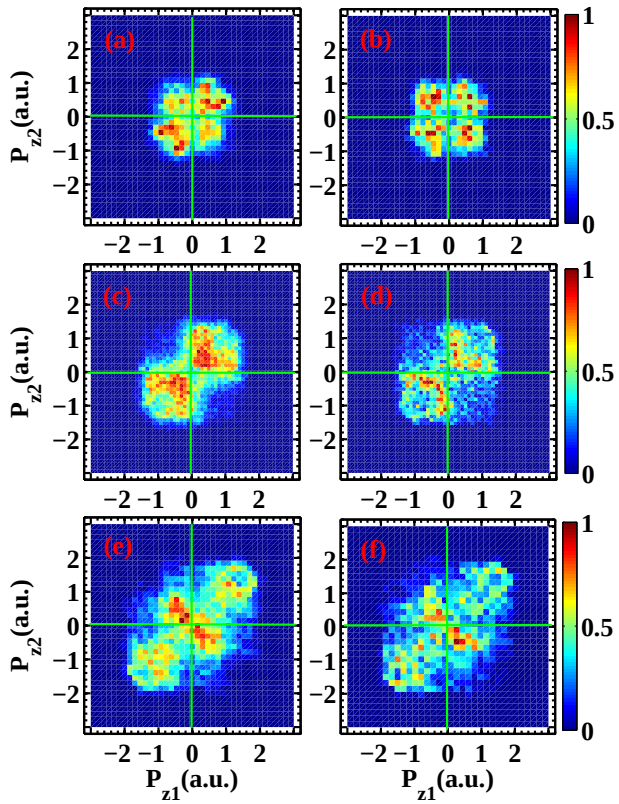

Fig. 1. The correlated electron momentum distributions in the direction parallel to the laser polarization for NSDI of nitrogen molecules at $I = 1.0 \times 10^{14} W/cm^2$. The wavelengths are (the first row) $\lambda = 800nm$, (the second row) $\lambda = 1200nm$ and (the third row) $\lambda = 1600nm$. In (a), (c) and (e), the molecules are aligned parallel to the laser polarization (ensemble sizes are 1 million). In (b), (d) and (f) the molecules are aligned perpendicular to the laser polarization (the ensemble sizes are 2 millions).

opposite hemispheres for the perpendicularly aligned molecules, which is consistent with the experimental results [28]. Our statistic shows that for the 800-*nm* pulses the proportions of electron pairs emitted into the same hemisphere are 60% and 50% for the parallel and perpendicular molecules, respectively. However, for the 1200 nm and 1600 nm, the correlated behavior of the electron pairs is independent on the molecular alignment. For the 1200-*nm* pulses the proportions of electron pairs emitted into the same hemisphere are 68% and 66% for the parallel and perpendicular molecules, respectively. And for the 1600-*nm* pulses, the proportions are 61% (parallel molecules) and 59% (perpendicular molecules). This means that the effect of molecular alignment on the correlated behavior of electron pairs is much weaker in the MIR regime than that in the NIR regime.

The responsible microscopic electron dynamics of the alignment-independent electron correlations at the long-wavelength regime can be revealed by back analysis of the doubly ionized trajectories. Tracing the classical DI trajectories allows us easily to determine the recollision time and the ionization time. For each DI trajectory, the recollision time is defined as the instant of the closest approach after first departure of one electron from the parent ion. The final ionization time is defined to be the instant when the energy of electron becomes positive for

#171495 - $15.00 USD Received 29 Jun 2012; revised 3 Aug 2012; accepted 6 Aug 2012; published 10 Aug 2012

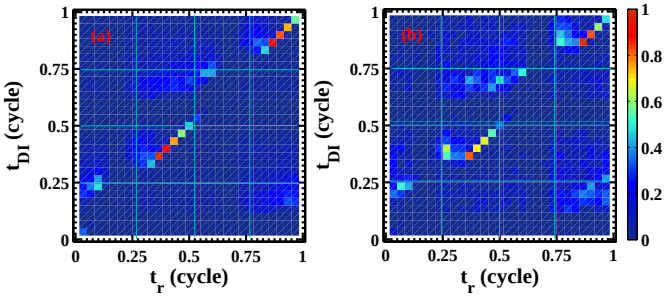

Fig. 2. Laser phase at double ionization time t_{DI} versus the phase at recollision time t_r (in laser cycle). (a) The molecules are aligned parallel to the laser polarization. (b) The molecules are aligned perpendicular to the laser polarization.

the first time, where the energy of the each electron contains the kinetic energy, potential energy of the electron-ion interaction and half electron-electron interaction repulsion. Figure 2 shows the laser phase t_{DI} (in cycles) at time of DI versus laser phase t_r at recollision [33] for the laser wavelength λ =1200 *nm*. Figures 2(a) and 2(b) correspond to the molecules aligned parallel and perpendicular to the laser polarization, respectively. It is clearly seen that most of recollisions occur in the time range 0.3T-0.5T (or 0.8T-1.0T, where the T is the laser cycle), just before the zero crossing of the field for both molecular alignments. It is consistent with the prediction of the simple-man model [18]. As shown in Fig. 2, the dominant part of the population are along the diagonal $t_{DI} = t_r$, which implies that most of DIs occur immediately after the recollision for both molecular alignments. This behavior is different from that in the NIR regime, where a significant part of the DI trajectories are ionized with a considerable time delay after recollision [29]. For the perpendicular molecules, the proportion of the delayed DI is larger than that for the parallel molecules, thus more electron pairs emit into the opposite hemispheres [29]. In the MIR wavelength, as shown in fig. 2, for both alignments NSDI are dominated by recollision ionization (RCI, where the second electron ionizes directly by the recollision of the first electron).

Now we further investigate the effect of the laser wavelength on the ion longitudinal momentum distribution. Figure 3 displays the longitudinal momentum spectra from NSDI of N_2 with the laser wavelengths of 800 *nm* (a), 1200 *nm* (b) and 1600 *nm* (c), respectively. The laser intensities are chosen to be (a) $2.25\times10^{14}W/cm^2$, (b) $1.0\times10^{14}W/cm^2$ and (c) $0.563\times10^{14}W/cm^2$, respectively, so that the ponderomotive energy for the three wavelengths is the same. The spectra in Fig. 3 are plotted in units of $\sqrt{U_p}$, where U_p is the ponderomotive energy. For 800-*nm* pulses, the spectrum exhibits a wide single-hump structure and it is well consistent with the experimental result [40]. When the wavelength increases to 1200 *nm*, the single-hump structure evolves into a double-hump structure [see Fig. 3(b)]. This double-hump structure becomes more pronounced as the wavelength further increases [see Fig. 3(c)]. These results agree excellently well with the experimental observations [25, 26].

To give an overall understanding of evolution of the ion momentum spectra, we analyze the time lag between DI and recollision for different laser wavelengths. Figure 4 shows the total faction of double ionization versus delay time between DI and recollision. In Fig. 4(a) the delay time are plotted in units of optical cycle. For 800-*nm* pulses, about 40% of the DI occurs within 0.25T after recollision, meaning that most of the DI occurs through RESI. For the 1200-nm pulses, about 50% of the DI occur within 0.25T and this proportion is 60% for the 1600-nm pulses, meaning that more and more DIs occur through RCI. Figure 4(b) also shows

#171495 - $15.00 USD Received 29 Jun 2012; revised 3 Aug 2012; accepted 6 Aug 2012; published 10 Aug 2012

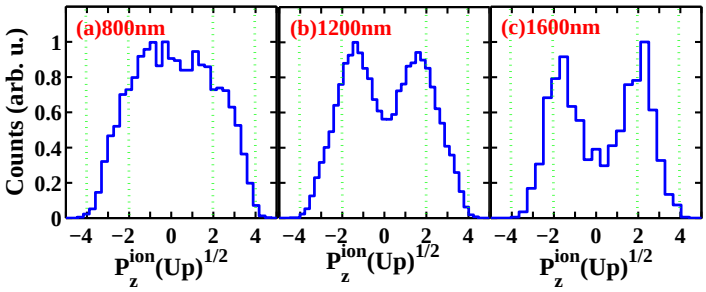

Fig. 3. The longitudinal momentum distributions of N_2^{2+} for different wavelengths, as indicated in each plot. The laser intensities are chosen to be (a) $2.25 \times 10^{14} W/cm^2$, (b) $1.0 \times 10^{14} W/cm^2$ and (c) $0.563 \times 10^{14} W/cm^2$, respectively, so that the ponderomotive energy for the 800-*nm*, 1200-*nm* and the 1600-*nm* pulses is the same (U_p=0.49 a.u.). The distributions are plotted in units of $\sqrt{U_p}$. The ensemble sizes are (a) and (b) 1 million and (c) 2 millions. Molecules are aligned parallel to the laser polarization.

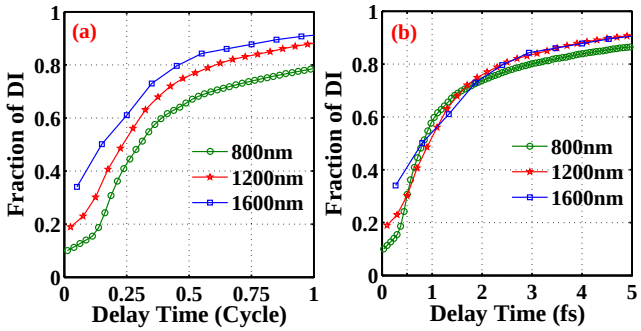

Fig. 4. Accumulated fraction of double ionization events versus time delay between closest recollision and double ionization. The delay time are plotted in units of (a) optical cycle and (b) femtosecond (fs).

the total faction of double ionization versus delay time, but the delay time is given in units of femtosecond. It can be seen that for the longer wavelengths the "absolute" delay time is also short than that of the shorter wavelength. This "absolute" delay time can been considered as the thermalization time [41]. This result means that for the longer wavelength pulses, the electrons are thermalized more quickly. This further indicates that at the long wavelength DI occurs more likely through RCI process and the second electron releases more quickly. The enhancement of the RCI process leads to the shape of the doubly charged ion spectrum evolving from a single-hump structure at NIR regime into a double-hump structure at MIR regime [25, 26].

The wavelength-dependent contribution of the RCI pathway can be qualitatively understood as follows. For a fixed ponderomotive energy, the electric field for the shorter wavelength is stronger than those of the longer wavelengths. Thus, after recollision, the ionization probability of the excited N_2^+ is higher for the shorter wavelength. While at the longer wavelengths, the ionization probability of the excited ion is lower because of the lower laser intensity. Thus, the RECI pathway is suppressed as compared to the case of the short wavelength. Consequently, NSDI is more dominated by the RCI pathway at the longer wavelengths. In ref. [25], Alnaser

#171495 - $15.00 USD Received 29 Jun 2012; revised 3 Aug 2012; accepted 6 Aug 2012; published 10 Aug 2012

et al. proposed that the ion momentum structure could be estimated by the scaling parameter $\alpha = I_p^3/\omega^2$ (I_p and ω are the ionization energy and laser frequency, respectively). They found that the dip structure in the momentum spectrum was more prominent for the higher value of α. Obviously, our results above are consistent with the analysis of Alnaser *et al.*

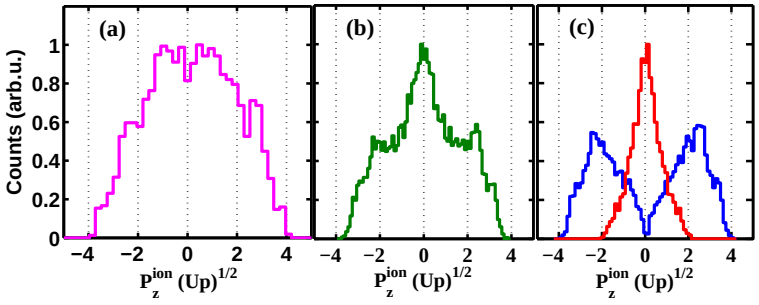

Fig. 5. The longitudinal momentum distributions of N_2^{2+} ion with the wavelength $\lambda = 1600nm$ at the intensity (a) $I = 0.8 \times 10^{14} W/cm^2$ and (b) $I = 1 \times 10^{14} W/cm^2$. The distributions of panel (b) are classified based on whether the electron pairs emit into the same hemisphere (blue solid curve) or the opposite hemispheres (red solid curve). The ensemble size is 1 million. The molecules are aligned parallel to the laser polarization.

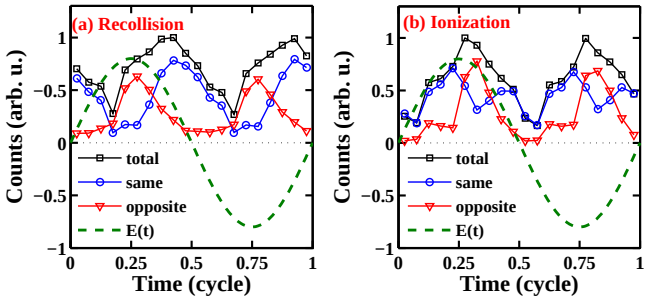

Fig. 6. Counts of the trajectories versus laser phase at (a) recollision and (b) final ionization of the second electrons. The black curves include all double ionization trajectories. The blue curves represent trajectories where the two electrons emit into the same hemisphere. The red curves denote trajectories where the two electrons emit into the opposite hemispheres. Molecules are aligned parallel to the laser polarization. The laser field is also shown (the green dashed curves). The laser parameters are $\lambda = 1600nm$, $I = 1 \times 10^{14} W/cm^2$.

In order to explore the intensity influence on the electron dynamics of the molecular NSDI in the MIR regime, we consider the higher laser intensities $0.8 \times 10^{14} W/cm^2$ and $1.0 \times 10^{14} W/cm^2$ for the 1600-*nm* pulses in Fig. 5. Comparing with Figs. 3(c) and 5(a), one can easily find that the valley of the ion longitudinal momentum distribution is filled up with the increase of the laser intensity. There is only a very shallow valley in the ion longitudinal momentum distribution for $0.8 \times 10^{14} W/cm^2$ [see Fig. 5(a)]. When the laser intensity further increases, the ion momentum spectrum exhibits a triple-hump structure [see Fig. 5(b)], which is different from the case at the lower intensity where it is a clear double-hump structure [see Fig. 3(c)]. In fig. 5(c) we divide the DI populations of fig. 5(b) into two parts: the electron pairs in the same (blue solid curve) and opposite (red solid curve) hemispheres. As shown in the Fig.

#171495 - $15.00 USD Received 29 Jun 2012; revised 3 Aug 2012; accepted 6 Aug 2012; published 10 Aug 2012

5(c), the central peak originates from the populations in the opposite hemispheres. To explore the responsible dynamics process for the triple-hump structure of the doubly charged ion momentum spectrum, we examine the laser phase at recollision and double ionization. Figures. 6(a) and 6(b) show the laser phase at recollision and at final ionization of the second electrons, respectively. For the DI populations in the same hemisphere, most recollisions occur before the zero crossing of the laser field [see the blue curve in Fig. 6(a)] and the relevant DIs occur near zero crossing of the laser field or before the first maximum of field after recollision [see the blue curve in Fig. 6(b)]. These results indicate that these electrons escape within a quarter laser cycle after recollision, and thus the electron pairs release into the same direction [4, 33]. While for the DI populations in the opposite hemispheres, most of recollisions [see the red curve in Fig. 6(a)] and DIs [see the red curve in Fig. 6(b)] occur near the maximum of the laser field. After recollision, the electron pairs emit into opposite directions because the laser field only provides a small drift momentum [4, 33]. This process results in a considerable proportion of opposite electron pairs at the higher intensity and thus the additional central peak in the momentum spectrum.

4. Conclusion

In summary, with the 3D fully classical ensemble model, we have investigated correlated electron dynamics in NSDI of N_2 by the MIR laser pulses. Our numerical results show that the correlated behavior of the two electrons from NSDI in the MIR regime is independent of the molecular alignment, contrary to the case in the NIR regime where the electron correlations exhibit a strong alignment dependence [28]. The longitudinal momentum spectra of the doubly charged ions exhibits a wide single-hump structure at the NIR regime. While in the MIR regime, the ions momentum spectra displays a double-hump structure and this double-hump shape becomes more pronounced as the wavelength increases, which is well consistent with the experimental results [25, 26]. Back analysis reveals that the RCI mechanism dominates NSDI for both alignments at the MIR regime, and thus for both alignments the electron pairs involved in NSDI more are likely to escape into the same hemisphere, leading to the alignment-independent electron correlation. The enhancement of contribution of the RCI also results in the double-hump structure of ions momentum spectra, which becomes more pronounced as the wavelength further increases because the contribution of RCI further increases. Additionally, in the MIR regime, the shape of the longitudinal momentum spectrum of N_2^{2+} changes from doublet to triplet as the intensity increases.

Acknowledgment

This work was supported by the National Science Fund for Distinguished Young Scholars under Grant No. 60925021, National Natural Science Foundation of China under Grant No. 11004070, and the 973 Program of China under Grant No. 2011CB808103.

#171495 - $15.00 USD Received 29 Jun 2012; revised 3 Aug 2012; accepted 6 Aug 2012; published 10 Aug 2012